Structural Investigation of Orthorhombic-to-Hexagonal Phase Transition in Polyethylene Crystal: The Experimental Confirmation of the Conformationally Disordered Structure by X-ray Diffraction and Infrared/Raman Spectroscopic Measurements

Kohji Tashiro,* Sono Sasaki, and Masamichi Kobayashi

Department of Macromolecular Science, Graduate School of Science, Osaka University, Toyonaka, Osaka 560, Japan

Received February 29, 1996; Revised Manuscript Received August 5, 1996[⊗]

ABSTRACT: Structural changes in the orthorhombic-to-hexagonal phase transition of polyethylene crystal has been investigated by measuring the differential scanning calorimetry, X-ray diffraction, and infrared and Raman spectra for the geometrically-constrained ultradrawn samples in the course of heating up to the melting temperature. The infrared and Raman spectral patterns characteristic of the hexagonal phase have been confirmed. In particular, the bands characteristic of the disordered short trans segments (shorter than five CH_2 units) and the bands of the kink or double gauche linkages have been detected definitely. The degree of orientation of the averaged chain axis, as detected from the temperature dependence of the X-ray fiber diagram, was reserved well enough even in the hexagonal phase, while the orientational degree of the methylene units, as detected from the polarized infrared spectral measurement, was found to be lowered appreciably. This finding, combined with the observation of the trans and gauche bands, has confirmed experimentally and definitely the existence of the conformationally disordered chains in the hexagonal phase.

Introduction

Polyethylene (PE) is one of the basically important polymers from both the industrial and scientific point of view. Among the various characteristic features of PE, the structural change occurring in the melting, crystallization, and/or phase transition may be a quite significant research theme because many physical properties of PE are associated with the aggregation state of the crystalline and amorphous phases and also with the inner structure of the crystallites. In the crystallization process, for example, the disordered chains change their structure to the regular conformation in the crystalline phase. The crystallization temperature is dependent upon the external condition and increases gradually as the hydrostatic pressure is increased, for example. As the temperature is decreased from the melt under such high pressure condition, the PE crystallizes firstly to the hexagonal phase and then to the normal orthorhombic phase.[1−7] This hexagonal phase plays an important role as an intermediate phase in the crystallization process from the melt to the extended chain crystal.[8] The structure of the hexagonal phase was investigated by X-ray diffraction[3,5,9] and Raman spectral measurements.[10] According to the X-ray diffraction study under the high-temperature and high-pressure conditions, the packing structure of the chains is appreciably disordered and the observation of the diffuse reflection corresponding to the repeating period of 2.3 Å suggests the existence of conformationally disordered chain.[9] But the concrete description of the disordering in the molecular chain conformation has not yet been given enough clearly. The Raman spectra were taken for the high-pressure hexagonal phase: the crystallization sensitive trans-zigzag bands were found to decrease the intensity remarkably in the hexagonal phase.[10] Such vibrational spectral data may give us concrete information on the conformational disorder of the chains. Unfortunately, however, the data reported so far are not persuasive because of their low signal-to-noise ratio. Besides, no infrared spectral data, which would give us structural information as useful as that from Raman spectra, have been reported concerning the hexagonal phase of PE. This situation is quite a contrast to the case of *n*-alkanes, for which the extensive spectroscopic study was made for the hexagonal rotator phase.[11−19] In this way, the structural information on the hexagonal phase has not yet been satisfactory enough to clarify the essential feature of the orthorhombic-to-hexagonal phase transition. Wunderlich et al. carried out the molecular dynamics calculation for the hexagonal phase and proposed the idea of the conformationally-disordered crystal phase (condis phase) for the hexagonal phase.[20−22] But they did not check the calculated results by comparing them with the experimental data of polyethylene because of a lack of detailed reports on the conformational distribution in the hexagonal state.

The limited number of reports may be due to the difficulty of performing the experiments under such severe conditions as high temperature and pressure. The orthorhombic-to-hexagonal phase transition can be observed also for the ultradrawn high-modulus PE samples subjected to high tensile stress.[23−28] For example, the X-ray diffraction and differential scanning calorimetry (DSC) data revealed the clear two-step transition from the orthorhombic phase to the hexagonal phase and to the melting state. These data could be obtained under an atmospheric pressure by using the highly oriented PE samples which were wound tightly around some metal holder. This type of measurement is easier and does not require the technically complicated high-temperature and high-pressure equipment to detect the orthorhombic-to-hexagonal phase transition. This situation encouraged us to carry out the investigation of structural features of the hexagonal

[⊗] Abstract published in *Advance ACS Abstracts,* October 15, 1996.

S0024-9297(96)00333-6 CCC: $12.00

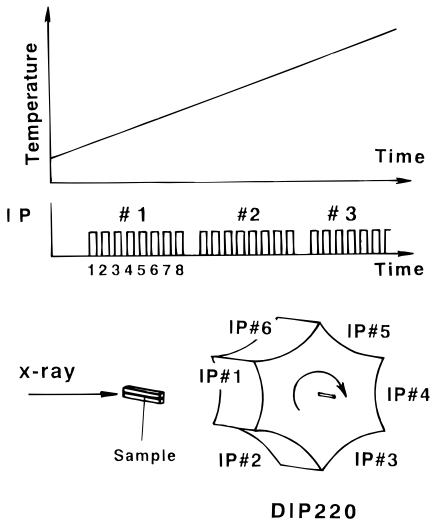

Figure 1. An illustrative principle of the time-resolved X-ray measurement by DIP220 imaging plate system.

phase because we could use the conventionally available experimental techniques under atmospheric pressure. In this paper, the structural features of the hexagonal phase will be discussed on the basis of the experimental data obtained by X-ray diffraction, Fourier-transform infrared (FTIR), and Raman (FT-Raman) spectral measurements made for the geometrically constrained PE samples. In the experiments we have another purpose, to check the usefulness of the imaging plate system for the time-resolved measurement of the two-dimensional X-ray diffraction patterns as well as the usefulness of the time-resolved FTIR/Raman spectroscopic system.

Experimental Section

Samples. In this study, the ultradrawn PE films used were obtained by the following procedures.[29,30] The 1.0 wt % ultrahigh molecular weight PE Hizex Million 240M (molecular weight $M_w = 1.5 \times 10^6$) was dissolved in decaline at 160 °C under the flow of nitrogen gas. This solution was poured rapidly into an ice−water bath, and the gel was precipitated. After being air-dried for 1 week, the gel was separated from the solution by filtration and air-dried further for 2 weeks. This dried gel was uniaxially drawn to ca. 120 times the original length in a silicone oil bath at 130 °C. The commercially available ultrahigh modulus polyethylene fiber Dyneema (M_w = ca. 3×10^6 and tensile modulus of ca. 130 GPa) was also used (supplied by Toyobo Co. Ltd.). Unoriented films of the ultrahigh molecular weight PE were obtained by slowly cooling the melt. Normal nonacosane (n-$C_{29}H_{60}$) was used as a reference.

Measurements. The DSC thermograms were measured by using a Seiko SSC/5200 differential scanning calorimeter at a heating rate of 1.0 °C/min.

The time-resolved wide-angle X-ray diffraction patterns were obtained by a MAC Science DIP220 imaging plate system with graphite-monochromatized Mo Kα radiation ($\lambda = 0.71073$ Å) generated by an M18XHF-SRA rotating anode X-ray generator operated at 50 kV and 200−300 mA. As shown in Figure 1, DIP220 is equipped with six imaging plates assembled like a drum. One plate (with 150 mm radius) can be translated horizontally in a step-scan mode and be divided into 1−16 sections by a rectangular slit. After the full screen of one plate is exposed, the drum is rotated by 60° and the next new plate is set to the camera position. In this way, the maximal 96 X-ray diffraction patterns can be taken successively.

The time-resolved measurements of the polarized or unpolarized infrared spectra were measured by a Bio-Rad FTS-60A/896 FT-IR spectrometer with an MCT detector. Rapid scan mode was employed at a rate of 0.15 s/scan with a spectral resolution of 2 cm^{-1}. The time step of the spectral measurement was 2.4−19.2 s/spectrum.

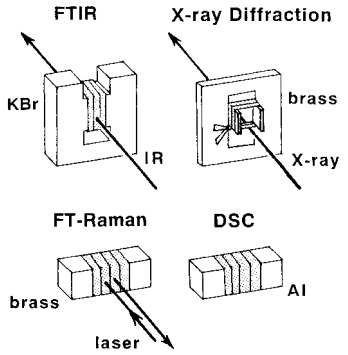

Figure 2. The sample holders used for the IR, Raman, X-ray diffraction, and DSC measurements.

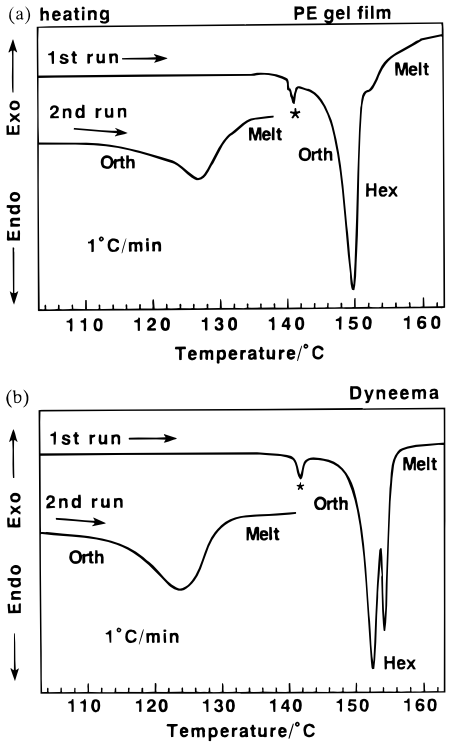

Figure 3. The DSC thermograms of (a) the constrained PE gel film and (b) Dyneema.

The Raman spectra were obtained at the resolution of 2 cm^{-1} by a Bio-Rad FTS Fourier transform Raman (FT-Raman) spectrometer equipped with a Nd:YAG laser ($\lambda = 1.064$ μm) as an excitation light source. A germanium detector was used to obtain the back-scattered Raman spectra.

Samples Holders. As already pointed out, the phase transition from orthorhombic to hexagonal phases of PE requires the tight constraint of the ultradrawn samples during heating to the melting temperature. This was attained by winding the samples tightly around the specially constructed holders appropriate for each measurement. Both ends of the thus wound samples were tied tightly. In Figure 2 are illustrated the holders used for this purpose, the materials of which were aluminum for DSC, KBr single crystal for FTIR, and brass for FT-Raman and X-ray diffraction measurements.

Separation of the Overlapped Infrared Bands. In order to evaluate the integrated intensity of each component in the overlapped infrared bands, the curve resolution was performed thoroughly. The band component was assumed to be a weighted mixture of the Lorentzian and Gaussian functions and the variables (the relative weight of these two functions, the height, the width, and the peak position) were adjusted by a nonlinear least-squares method so that the totally summed spectral profile was fitted to the observed

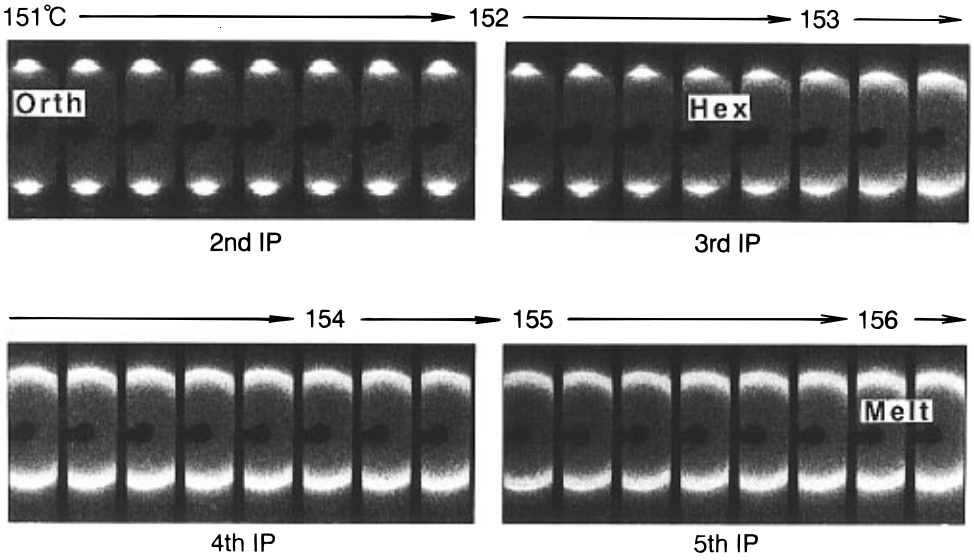

Figure 4. Time dependence of the X-ray diffraction pattern of the constrained Dyneema measured in the heating process by the DIP220 imaging plate system. The exposure time is 10 s/shot. The interval between the successive two plates is 14 s.

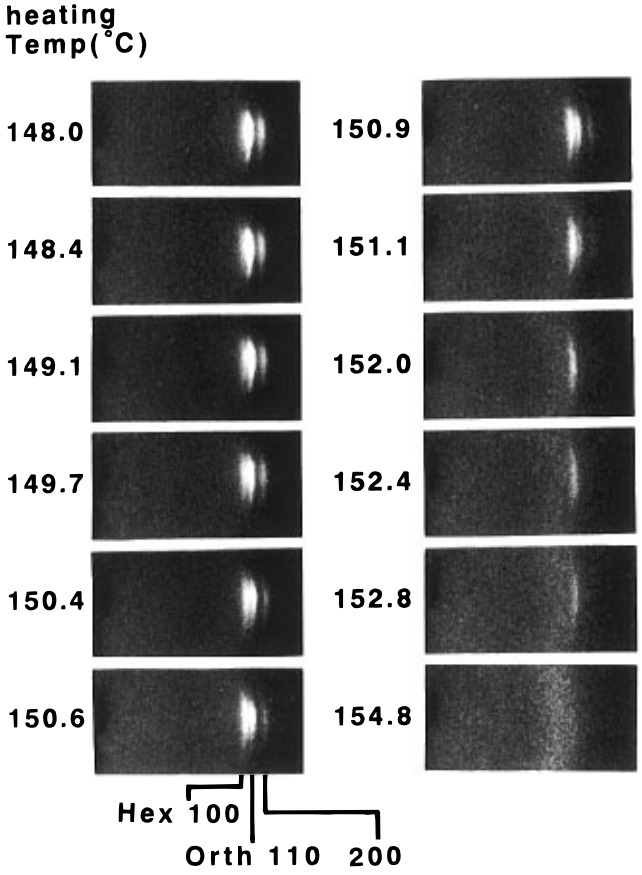

Figure 5. Temperature dependence of the X-ray diffraction pattern measured for the constrained PE gel film in the heating process by the DIP220 imaging plate system: Orth, the orthorhombic phase; Hex, the hexagonal phase.

pattern as well as possible. The used program was that installed in the Bio-Rad FTS-60A/896 FT-IR spectrometer.

Results and Discussion

Characterization of the Transition by DSC, X-ray Diffraction, and Infrared/Raman Spectroscopic Measurements. DSC. DSC measurements were carried out in order to evaluate the temperature of the orthorhombic−hexagonal phase transition which should occur in the geometrically constrained ultradrawn PE samples. This information is very useful as a guide line for performing the X-ray diffraction and infrared and Raman spectral measurements. Figure 3a shows the DSC thermograms obtained for the constrained PE gel film at the heating rate of 1 °C/min. The peak indicated by an asterisk corresponds to the melt of the incompletely constrained parts of the sample. The two endothermic peaks are observed between 146 and 154 °C, which correspond, respectively, to the transitions from the orthorhombic phase to the hexagonal phase and to the melt.[23−28] This is quite contrast to the thermogram measured for the strain-free sample, which shows only one transition peak from the orthorhombic phase to the melt (see the curves of the second run in Figure 3). As for Dyneema (Figure 3b), the essential feature of the DSC thermogram is the same as that of the PE gel film, but the temperature region and the relative intensity of the two peaks are much different. This difference will be discussed in detail in a later section.

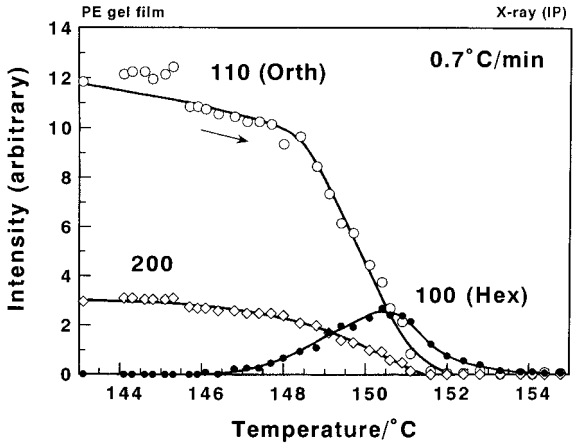

Figure 6. Temperature dependence of the integrated intensity of the X-ray reflections measured for the constrained PE gel film at the heating rate of 0.7 °C/min: Orth, the orthorhombic phase; Hex, the hexagonal phase.

X-ray Diffraction. The time-resolved X-ray diffraction measurements were performed for the sample heated continuously at a constant rate of ca. 0.7 °C/min. The sample must be bound tightly to allow observation of the orthorhombic-to-hexagonal phase transition, but

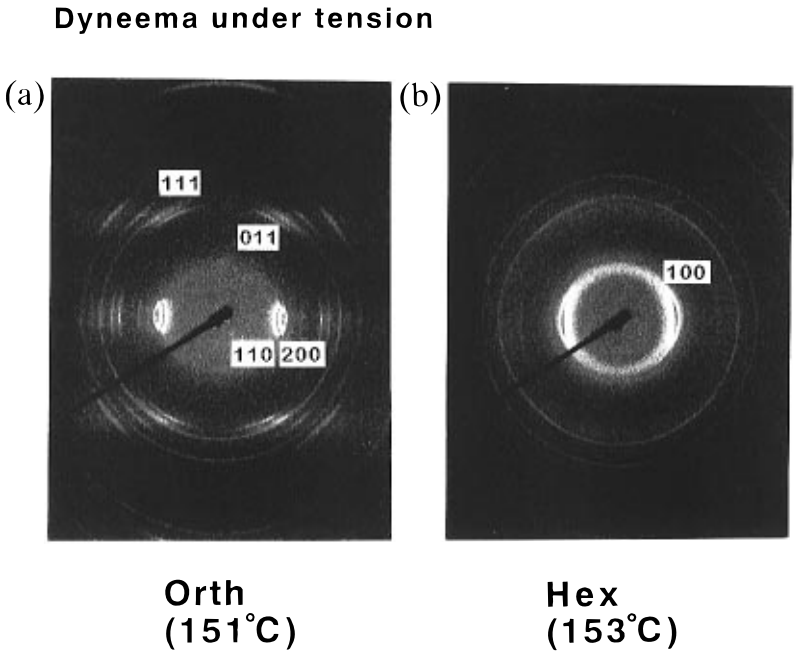

Figure 7. The X-ray fiber patterns of (a) the orthorhombic phase and (b) the hexagonal phase of the constrained Dyneema.

the binding part might be slackened during heating close to the melting point, so the measurement should be made rapidly before such a slackening of the sample. This concerned other researchers previously,[23−28] and we also carried out the experiment at a relatively rapid heating rate. But, while making measurements we noticed that this is not necessarily an important matter and the orthorhombic-to-hexagonal phase transition can be observed even at slow heating rate as long as the binding of the sample ends is made carefully and tightly.

The time dependencies of the X-ray diffraction pattern taken for Dyneema and the PE gel film are shown in Figures 4 and 5, respectively. The heating rate of the sample was 0.7 °C/min and the exposure time was 10 s with an interval of 1.5 s. As the temperature is increased to the phase transition region detected in the DSC thermograms, the intensity of the 110 and 200 reflections of the orthorhombic phase is decreased and the 100 reflection of the hexagonal phase begins to appear. With further increase of the temperature, the orthorhombic phase disappears finally and the hexagonal phase increases its intensity. In the higher temperature region, the reflection pattern gradually changes to the halo characteristic of the molten state. The integrated intensity of the reflections evaluated for the PE gel film (Figure 5) are plotted against the temperature as shown in Figure 6. The intensity exchange between the orthorhombic and hexagonal phases can be detected clearly around 146−154 °C, which corresponds well to the endothermic peak of the DSC curves shown in Figure 3. Figure 7 shows the X-ray fiber patterns of the orthorhombic and hexagonal phases measured for the constrained Dyneema. The equatorial reflections of the hexagonal phase remain sharp while the layer reflections become diffuse. This suggests that some degree of disordering occurs in the relative height of the neighboring chains, as pointed out through the analysis of the X-ray pattern of the hexagonal phase obtained under high-temperature and high-pressure conditions.[8] The observation of well-oriented sharp equatorial reflections indicates that the averaged orientation of the molecular chain axis is not changed much even in the hexagonal phase.

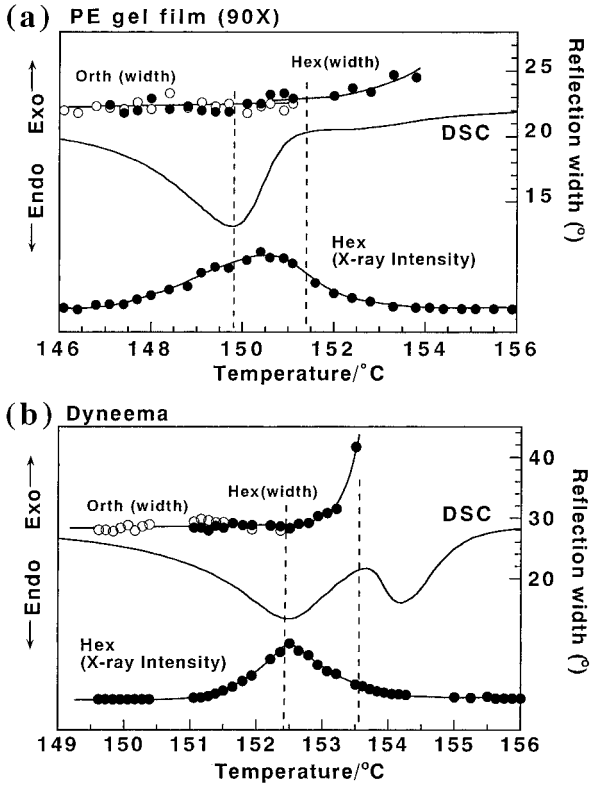

Figure 8. Temperature dependence of the full-width of the X-ray reflections (110 for the orthorhombic phase and 100 for the hexagonal phase) in comparison with the DSC thermograms and X-ray intensity change of the hexagonal phase (100 reflection). (a) gel film and (b) Dyneema samples.

In order to confirm this statement about the chain orientation in the hexagonal phase, we evaluated the degree of chain orientation from Figures 4 and 5, for which the full-widths of the reflections along the azimuthal direction were measured by actually viewing the profiles. The obtained temperature dependencies of the reflectional width measured for the orthorhombic 110 and hexagonal 100 reflections are plotted in Figure 8, where the data are compared with the DSC thermogram and the X-ray intensity change of the hexagonal 100

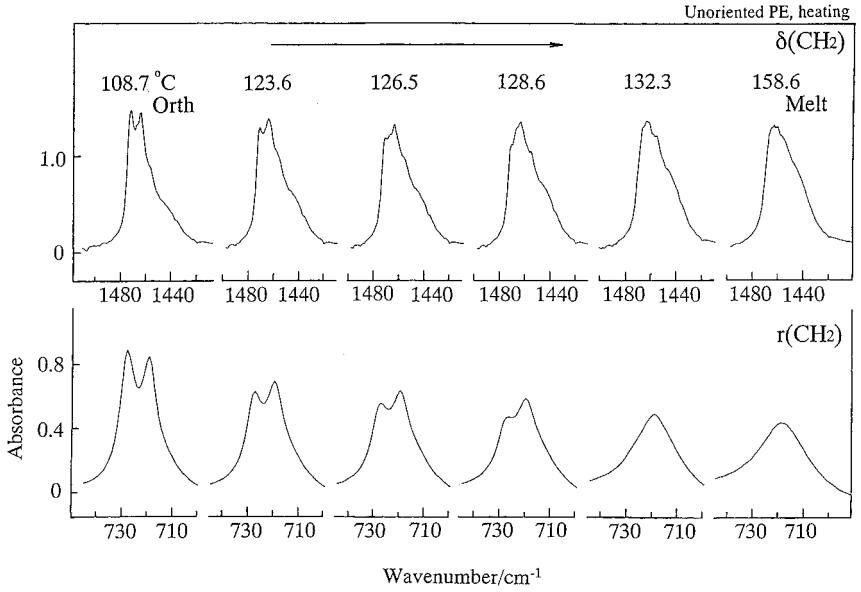

Figure 9. The infrared spectral change in the frequency region of the CH_2 (upper) bending and (lower) rocking modes measured for the unoriented PE film in the heating process.

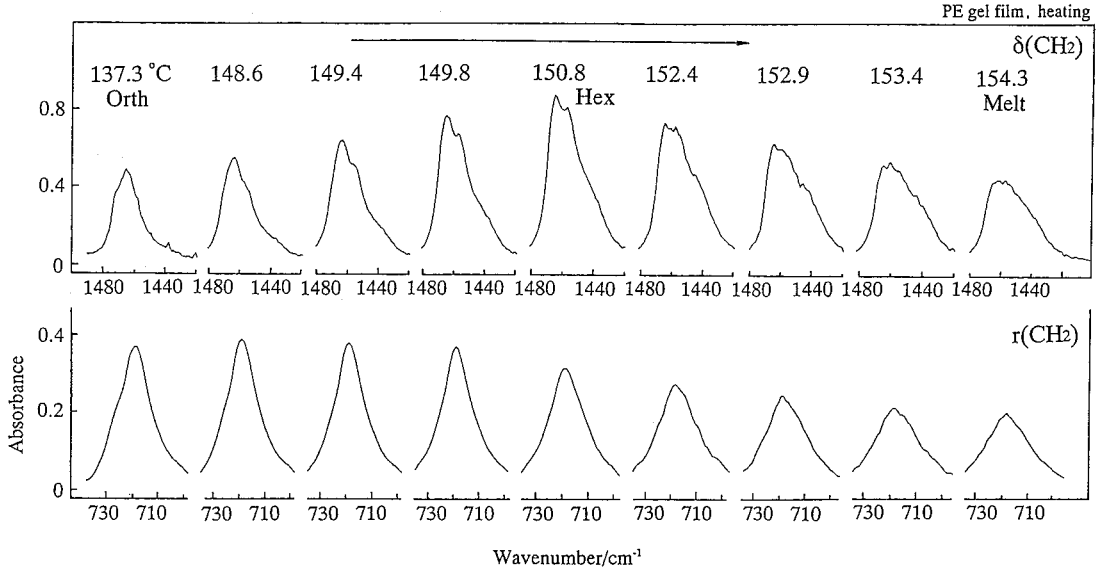

Figure 10. The infrared spectral change in the frequency region of the CH_2 (upper) bending and (lower) rocking modes measured for the constrained PE gel film in the heating process.

reflection. For example, in the case of Dyneema sample, the orthorhombic phase begins to disappear in the temperature region of 150−152 °C and the large endothermic peak is observed in the DSC thermogram and the intensity of the hexagonal phase increases, during which the full-width of the observed reflections or the chain orientation is not actually changed for both the orthorhombic and hexagonal phases. As the temperature is increased further to the melting region of 153.5−154 °C, the chain orientation becomes worse rapidly because of melting. Such a situation can also be observed for the case of gel film, as seen in Figure 8. In this case the transitional temperature from the orthorhombic-to-hexagonal phase is slightly lower than that of Dyneema used here, and so the decrease of the chain orientation is relatively low compared with the case of Dyneema. In any case, however, the chain orientation, as estimated from the X-ray diffraction data, may be said to be reserved well even in the hexagonal phase as long as the sample does not approach the melting region.

FTIR. In the IR measurement of the constrained sample, the film was wound tightly many times around the KBr holder, as illustrated in Figure 2. For the strain-free sample, the film was sandwiched between a pair of KBr plates. The time-resolved infrared spectra were measured during the heating process at 5 °C/min for the accumulation time of one spectrum of 19 s. The infrared spectral change in the frequency region of the CH_2 bending mode is shown in Figure 9 for the strain-free unoriented film. As the temperature increases, the intensity of the orthorhombic crystalline band (1471 cm^{-1}) decreases and the broad bands characteristic of the melt begin to appear instead. In the case of the constrained PE gel film, as shown in Figure 10, new bands appear around 1460−1470 cm^{-1} and the intensity increases remarkably, while the intensity of the orthorhombic crystalline band (1471 cm^{-1}) is decreased. In the higher temperature region, the intensity of these new bands decreases and the amorphous bands are observed intensely. The integrated intensity of these bands, after careful curve resolution, is plotted as a

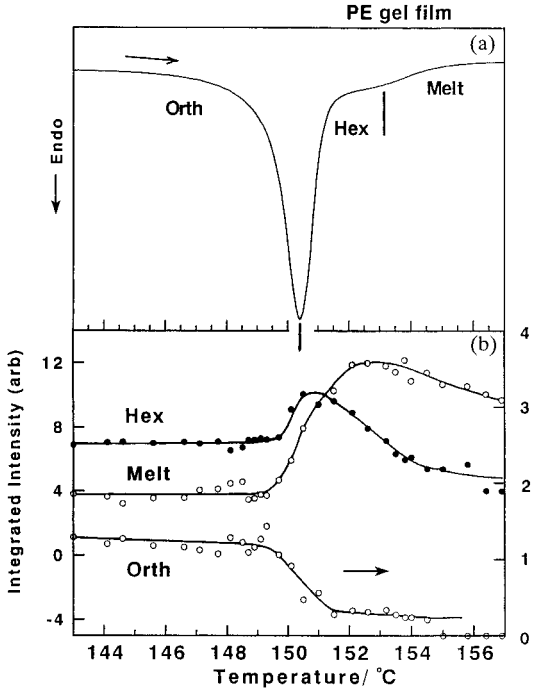

Figure 11. Comparison between (a) the DSC thermogram and (b) the integrated intensity of the infrared absorption bands for the constrained PE gel film: Orth, orthorhombic (1471 cm^{-1}); Hex, hexagonal (1466 cm^{-1}); Melt, (1433 cm^{-1}).

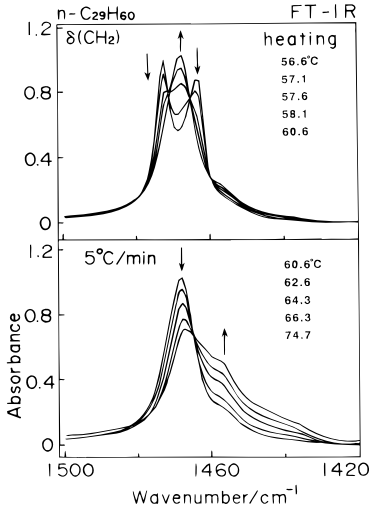

Figure 12. Temperature dependence of the infrared spectra of *n*-$C_{29}H_{60}$ in the frequency region of the CH_2 bending mode measured during the heating process.

function of temperature in Figure 11. The 1471 cm^{-1} band decreases and the 1466 cm^{-1} band increases in the temperature region where the orthorhombic–hexagonal phase transition is detected in the DSC curve. This means that the 1466 cm^{-1} band is considered to originate from the hexagonal phase. As shown in Figure 10, the infrared bands of similar behavior are observed also in the CH_2 rocking region: the band at 719 cm^{-1} was found to increase in intensity transiently during the intensity decrement of the orthorhombic-phase bands and then decrease down to the melt pattern. These behaviors of the infrared bands are very similar to those observed in the orthorhombic-to-hexagonal transition of the *n*-alkane crystal $C_{29}H_{60}$. As shown in Figures 12 and 13, in the transition temperature region the bands characteristic of the hexagonal rotator phase are observed to increase in intensity.[11–16] For example, in the CH_2 bending region (Figure 12), a new band

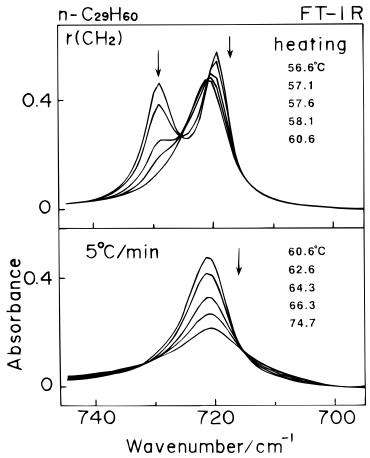

Figure 13. Temperature dependence of the infrared spectra of *n*-$C_{29}H_{60}$ in the frequency region of the CH_2 rocking mode measured during the heating process.

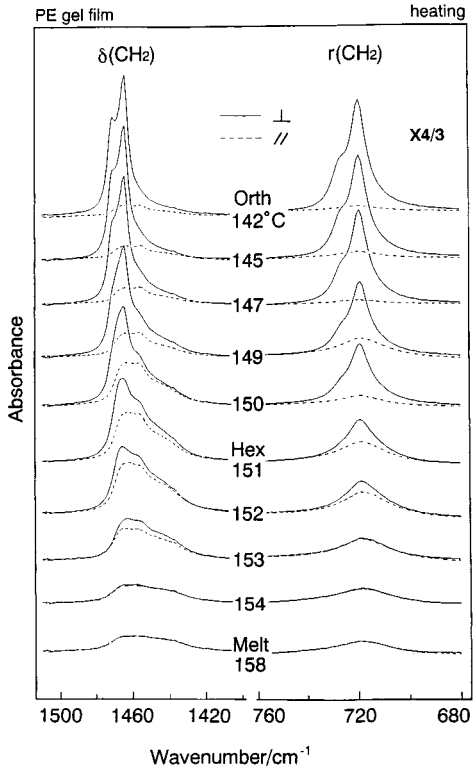

Figure 14. Temperature dependence of the polarized infrared spectra in the frequency regions of the CH_2 bending and rocking modes measured for the constrained PE gel film. ⊥ and ∥ denote that the electric vector of the incident infrared beam was perpendicular and parallel to the chain orientation direction, respectively.

begins to appear and increase in intensity at the center position (1468 cm^{-1}) between the two orthorhombic bands at 1463 and 1472 cm^{-1}. In the CH_2 rocking region (Figure 13), the 719 and 730 cm^{-1} bands decrease in intensity and the band at 721 cm^{-1} increases in intensity instead. Although the band positions are slightly different between PE and *n*-alkane (possibly because of the difference in the chain length), the behavior of the hexagonal bands is essentially the same.

The polarized infrared spectra were also measured for the constrained sample during heating as shown in Figure 14. The bands of the orthorhombic phase show quite clear dichroism even at such a high temperature as 142 °C. The spectral pattern at 151 °C, for example, is typical of the hexagonal phase and the bands still

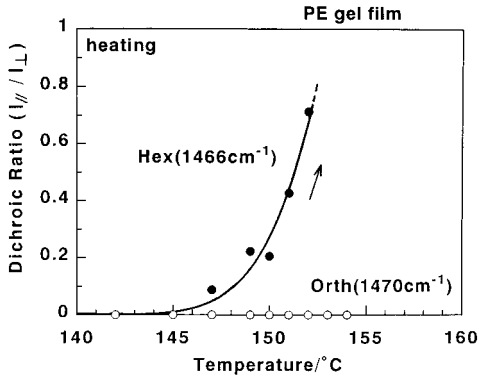

Figure 15. The temperature dependence of the dichroic ratio (R) for the orthorhombic (1471 cm^{-1}) and hexagonal (1466 cm^{-1}) bands measured for constrained PE gel film.

exhibit clear dichroism. But the parallel components (the broken line) increase the intensity, so the dichroic ratios are to some extent lower than those in the orthorhombic phase. The dichroic ratio (R) evaluated for the orthorhombic (1471 cm^{-1}) and the hexagonal (1466 cm^{-1}) bands is plotted against temperature in Figure 15, where the dichroic ratio R is defined as $R = I_{\parallel}/I_{\perp}$ and $I_{\parallel}$ is the integrated intensity of the parallel component and $I_{\perp}$ is that of the perpendicular component. In the orthorhombic-to-hexagonal transition region, the R of the hexagonal band rapidly approaches unity with increasing temperature. This relatively poor dichroic ratio in the hexagonal phase apparently contrasts the high degree of the orientation revealed by the X-ray diffraction pattern. These apparently contradictory experimental results between the IR and X-ray measurements can be interpreted reasonably: the orientation of the whole molecular chains is kept unchanged on average, but the CH_2 groups themselves are disordered in orientation. In other words, the molecular chain may be considered to change its conformation from the regular all-trans form to the disordered structure which is constructed by a random sequence of the trans and gauche rotational isomers. If this assumption of the conformational disorder is correct, then we should expect to be able to detect the "polarized" infrared bands characteristic of the gauche sequences. Figure 16 shows the temperature change of the infrared spectra in the CH_2 wagging modes. The 1366, 1306, and 1352 cm^{-1} bands increase their intensity remarkably in the hexagonal phase, with the clear parallel polarization being kept. The total intensity of these bands are plotted against the temperature in Figure 17, where we can observe the increase and decrease of these hexagonal bands in the phase transition temperature region. Following the vibrational analyses made for *n*-alkanes,[14–16] the 1366 and 1306 cm^{-1} bands may be assigned to the kink structure (...TTGT$\bar{G}$TT...) and the 1352 cm^{-1} band to a double gauche form (...TTGGTT...). In this way we have been able to identify the bands characteristic of the conformationally disordered hexagonal phase of PE. The main bands are listed as below.

1466 cm^{-1}	disordered trans segments
1366, 1306 cm^{-1}	kink (...TTGT$\bar{G}$TT...)
1352 cm^{-1}	double gauche (...TTGGTT...)

Raman Spectra. By measuring the infrared spectral pattern of the hexagonal phase we have been able to get some valuable information concerning the structural

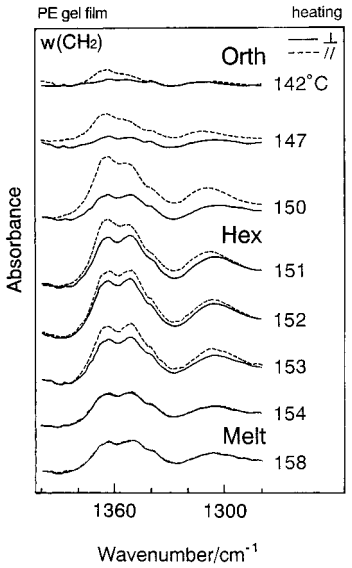

Figure 16. Temperature dependence of the polarized infrared spectra in the frequency region of the CH_2 wagging mode measured for the PE gel film: Orth, orthorhombic; Hex, hexagonal. ⊥ and || denote that the electric vector of the incident infrared beam was perpendicular and parallel to the orientation direction, respectively.

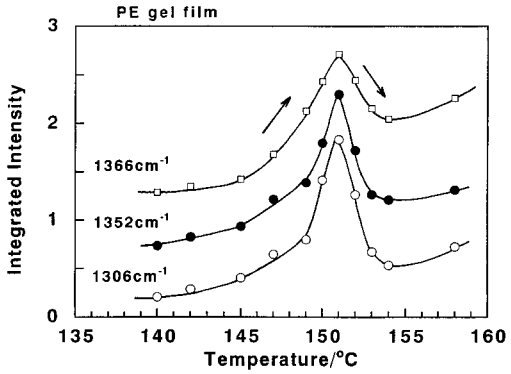

Figure 17. Temperature dependence of the integrated intensity of the CH_2 wagging bands characteristic of the conformationally disordered trans sequences: 1366 and 1306 cm^{-1}, kink form; 1353 cm^{-1}, double gauche form.[13–15] The above two curves are shifted upward by 0.5 each to avoid overlapping.

disordering attendant with the trans−gauche conformational change. In order to estimate the trans−gauche distribution in the chains, the Raman spectra were measured as a function of temperature, because the Raman bands were reported already to be sensitive to the trans-zigzag sequential length of the PE chains.[31] In Figure 18 are shown the Raman spectra of PE measured when strain-free and under tension. In the former case, the trans-zigzag bands decrease in intensity gradually with increasing temperature and disappear above the melting point. In the case of the constrained PE sample (Figure 18b), also, the trans-zigzag bands [for example, the symmetric and antisymmetric skeletal bond stretching modes ν_s(CC) and ν_{as}(CC)] decrease in intensity and the whole pattern becomes similar to that of the melt. But the intensity of these bands, which are assignable apparently to the molten state, increases in the temperature region of the orthorhombic-to-hexagonal phase transition and then decreases down to that of the melt. The frequency region of the CH_2 stretching modes also was found to exhibit such a transient increase of the Raman bands of the disordered structure.

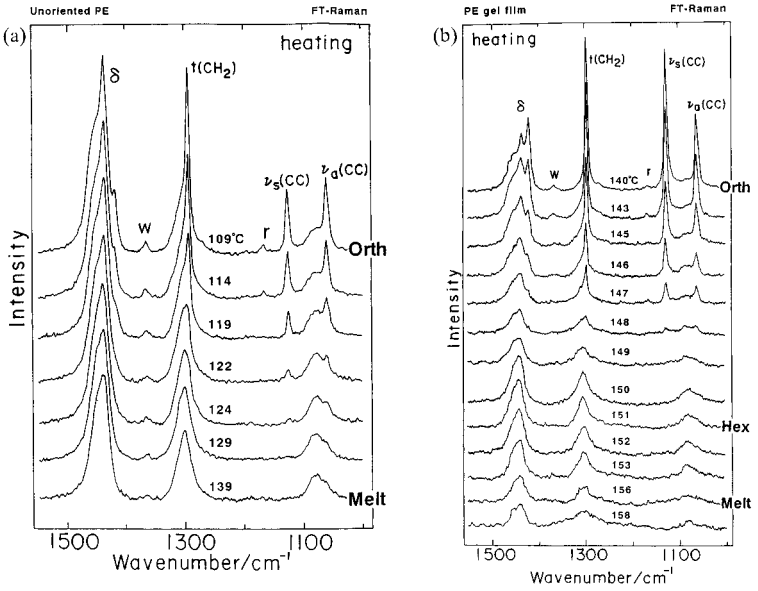

Figure 18. Temperature dependence of the FT-Raman spectra measured for (a) unoriented PE sample and (b) the constrained PE gel film.

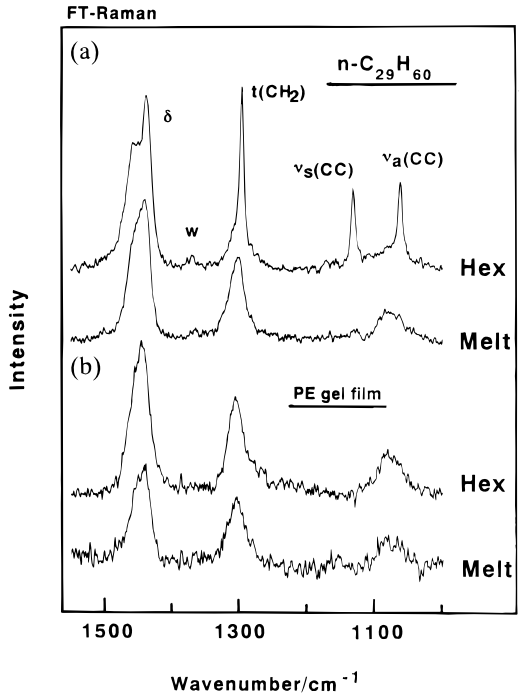

Figure 19. Comparison of the Raman spectra between the hexagonal phase and the melt measured for the PE gel film and n-$C_{29}H_{60}$.

In this way the whole spectral pattern of the hexagonal phase apparently cannot be distinguished from that of the molten state. Figure 19 compares the Raman spectra of the hexagonal phase of the PE gel film with those of the rotator phase of n-$C_{29}H_{60}$. The spectrum of the rotator phase of n-$C_{29}H_{60}$ shows the Raman bands at 1130 and 1062 cm^{-1}, which are characteristic of the trans-zigzag conformation. The rotator phase of n-alkane exists as a conformationally disordered phase consisting of mainly trans-zigzag chains with the gauche bonds near the ends (Figure 20);[11−13] in fact, the trans bands can still be observed even in the hexagonal phase. But, in the case of the PE sample, these trans-zigzag bands cannot be observed practically at all. Kobayashi et al. evaluated the critical sequence length for some regularity-sensitive Raman bands by using the random

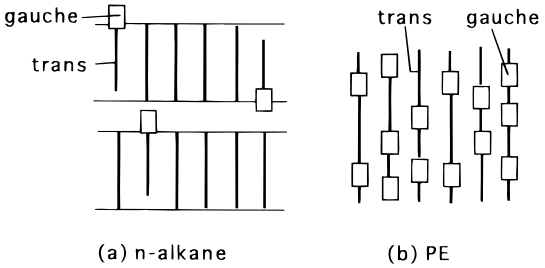

Figure 20. Illustrated structure of (a) the rotator phase of n-alkanes and (b) the hexagonal phase of PE.

Table 1. Critical Sequence Length (m) of Raman Bands for Planar−Zigzag PE Chains[31]

band/cm^{-1}	mode[a]	m CH_2 units
2883	$\nu_s(CH_2)$	4−6
1295	$t(CH_2)$	6
1170	$r(CH_2)$	18
1130	$\nu_s(CC)$	18
1062	$\nu_a(CC)$	6−8

[a] Vibrational modes: $\nu_s(CH_2)$, methylene symmetric stretching; $t(CH_2)$, methylene twisting; $r(CH_2)$, methylene rocking; $\nu_s(CC)$, symmetric stretching of skeletal CC bond; $\nu_a(CC)$, anti-symmetric stretching of skeletal CC bond.

copolymers of ethylene and deuterated ethylene, as listed in Table 1.[31] For example, the 1062 cm^{-1} band needs a trans-zigzag sequence of at least 6 to 8 methylene units to be observed. In the Raman spectra of the hexagonal phase, no such specified bands as indicated in Table 1 were observed, implying that the trans-zigzag sequence in the hexagonal phase may be five methylene units at most. Different from the rotator phase of n-alkanes, the gauche bonds are considered to distribute among the entire molecular chain, as evidenced by the similarity of the Raman spectra to those of the molten state and also by the observation of the CH_2 wagging infrared bands (Figure 16). In Figure 20 are shown the conceptional illustrations of the structure of the hexagonal phase of n-alkane and PE sample.

Structure of the Hexagonal Phase. From all the data of the X-ray diffraction and infrared and Raman spectra, the hexagonal phase may be considered to consist of the parallel packing of the conformationally disordered molecular chains in which the trans−gauche

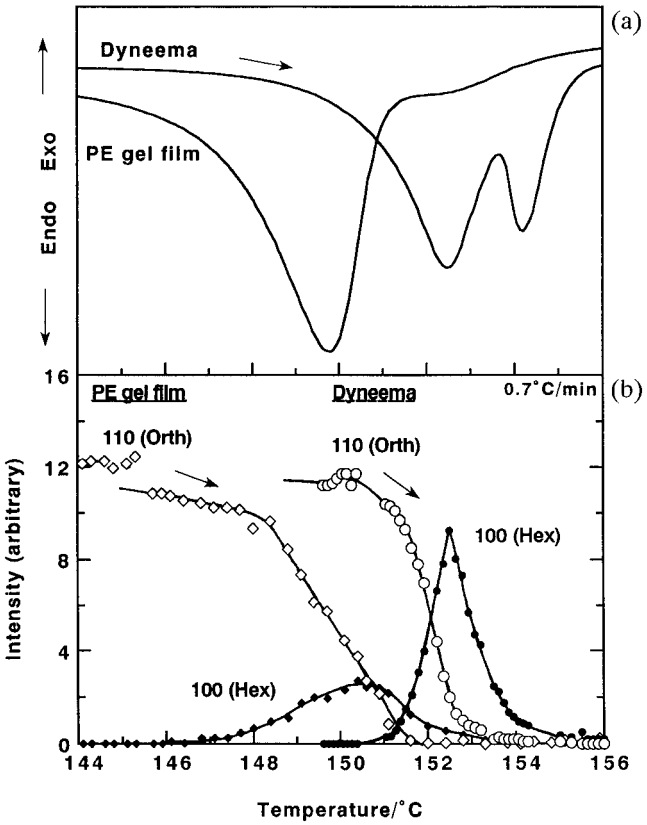

Figure 21. Comparison of (a) the DSC thermograms and (b) the integrated intensity of the X-ray diffraction between the constrained PE gel film and Dyneema: 110(Orth), the orthorhombic 110 reflection; 100(Hex), the hexagonal 100 reflection.

rotational isomers distribute randomly with the trans sequences shorter than five CH_2 units. This may be the first experimentally confirmed description of the concrete structural features of the hexagonal phase of PE. The structural image obtained from the present study may be reasonably applicable to that of the hexagonal phase generated under high-temperature and high-pressure conditions. Wunderlich et al. carried out the molecular dynamics simulation of the long alkane chain crystal at a high temperature. They estimated that the conformationally disordered (Condis) phase consists of essentially trans-zigzag chains with gauche defects of ca. 10%.[20−22] Judging from the infrared and Raman spectral data presented here, this value seems to be an underestimation. If we assume the statistically random distribution of the trans−gauche isomers with trans CH_2 sequences shorter than five units, the gauche content may be estimated higher than 20%. Anyway, however, it may be useful to carry out a molecular dynamics simulation in a quantitative manner to reproduce the actually observed X-ray diffraction and infrared and Raman spectral data of the hexagonal phase, the result of which will be published in the near future.

Factors Affecting the Phase Transitional Behavior. In the present study, we have noticed that the phase transitional behavior is affected more or less by the history of the used samples. In Figure 21a the DSC curves are compared between the constrained PE gel film and Dyneema. The DSC curve observed for Dyneema exhibits relatively sharp peaks during the orthorhombic-to-hexagonal phase transition, while a broad peak is observed for the PE gel film. The temperatures of these peaks are also different from each other. Corresponding to these DSC data, the temperature

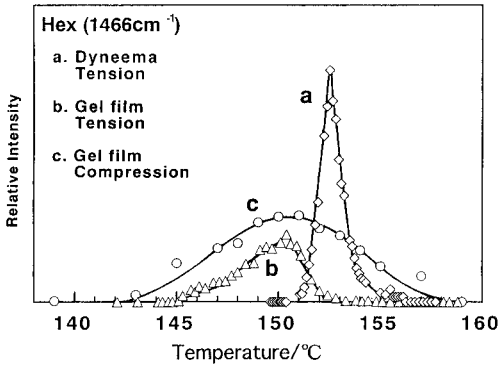

Figure 22. Comparison of the temperature dependence of the infrared band intensity characteristic of the hexagonal phase among (a) the constrained Dyneema, (b) the constrained PE gel film, and (c) the compressed PE gel film.

dependence of the X-ray intensity is also different, as shown in Figure 21b.

Such a difference in the transitional behavior can be noticed also for the different methods of constraining the samples. In the infrared spectral measurements, for example, the sample was wound tightly around a KBr holder: this method requires a skillful technique. We measured the infrared spectra also for the sample which was more easily prepared by compressing a piece of PE gel film into a KBr disk. In Figure 22 the integrated intensity of the 1466 cm^{-1} infrared band characteristic of the hexagonal phase is compared among the three types of samples: the tightly wound Dyneema, the tightly wound gel film, and the highly compressed gel film. The orthorhombic-to-hexagonal transition occurs in a wide temperature range for the compressed sample, which covers those of Dyneema and the tensioned gel film. In particular, in the case of Dyneema, the transition occurs in a narrow temperature region, as seen in Figure 22.

In this way the orthorhombic-to-hexagonal transition is dependent largely on the sample preparation as well as the constraining condition during heating. This difference in the transitional behavior might originate from the stress distribution within the sample being different among the used samples. In other words, by utilizing the difference in the phase transitional behavior, we might obtain useful information on the stress distribution within the constrained PE samples.

Conclusions

In this paper the orthorhombic−hexagonal phase transition of the geometrically constrained ultrahigh modulus PE samples was traced during the heating process by time-resolved X-ray diffraction and FTIR/Raman methods. In particular, the infrared spectra characteristic of the hexagonal phase have been obtained experimentally for the first time. The analysis of the X-ray diffraction and the polarized FTIR spectra indicated that the CH_2 groups are orientationally disordered in the hexagonal phase because of the trans−gauche conformational exchange, whereas the averaged orientation of the whole molecular chains is reserved enough well, as long as the temperature is not close to the melting region (Figure 8). The existence of kink and double gauche structures could be proved experimentally. The Raman spectrum of the hexagonal phase was found to be much similar to that of the molten state. By analyzing the Raman spectrum of the hexagonal phase, the trans sequential length in the disordered

chains was estimated to be shorter than five CH_2 units at most. On the basis of all of the data obtained experimentally, the hexagonal phase has been concluded to consist of the parallel packing of the conformationally disordered molecular chains which are constructed by the randomly arrayed trans and gauche sequences. In other words, we have for the first time confirmed experimentally the hexagonal phase to be the "condis phase".

Acknowledgment. The authors wish to thank Toyobo Co. Ltd. for kindly supplying the ultradrawn PE samples Dyneema.

References and Notes

(1) Bassett, D. C.; Khalifa, B. A.; Turner, B. *Nature* **1972**, *239*, 106.
(2) Bassett, D. C.; Turner, B. *Nat. Phys. Soc.* **1972**, *240*, 146.
(3) Bassett, D. C.; Block, S.; Piermarini, G. J. *J. Appl. Phys.* **1974**, *45*, 4146.
(4) Yasuniwa, M.; Nakafuku, C.; Takemura, T. *Polym. J.* **1973**, *4*, 526.
(5) Yasuniwa, M.; Enoshita, R.; Takemura, T. *Jpn. J. Appl. Phys.* **1976**, *15*, 1421.
(6) Yasuniwa, M.; Yamaguchi, M.; Nakafuku, A.; Tsubakihara, *Polym. J.* **1990**, *22*, 411.
(7) Schul'gin, A. I.; Aulov, V. A. *Vysokomol. Soyed.* **1991**, *A33*, 1576.
(8) Rastogi, S.; Hikosaka, M.; Kawabata, H.; Keller, A. *Macromolecules* **1991**, *24*, 6384.
(9) Yamamoto, T.; Miyaji, H.; Asai, K. *Jpn. J. Appl. Phys.* **1977**, *16*, 1891.
(10) Tanaka, H.; Takemura, T. *Polym. J.* **1980**, *12*, 355.
(11) Strobl, G.; Ewen, B.; Fischer, E. W.; Piesczek, W. *J. Chem. Phys.* **1974,** *61*, 5257.
(12) Ewen, B.; Fischer, E. W.; Piesczek, W.; Strobl, G. *J. Chem. Phys.* **1974**, *61*, 5265.
(13) Ewen, B.; Strobl, G. R., Richter, D. *J. Chem. Soc., Faraday Discuss.* **1980**, *69*, 19.
(14) Snyder, R. G.; Maroncelli, M.; Qi, S. P.; Strauss, H. L. *Science* **1981**, *214*, 188.
(15) Maroncelli, M.; Qi, S. P.; Strauss, H. L.; Snyder, R. G. *J. Am. Chem. Soc.* **1982**, *104*, 6327.
(16) Kim, Y.; Strauss, H. L.; Snyder, R. G. *J. Phys. Chem.* **1989**, *93*, 7520.
(17) Pyckaert, J. P.; Mcdonald, I. R.; Klein, M. L. *Mol. Phys.* **1989**, *67*, 957.
(18) King, H. E., Jr.; Sirota, E. B.; Singer, D. M. *J. Phys. D: Appl. Phys.* **1993**, *26*, B133.
(19) Sirota, E. B.; King, H. E., Jr.; Singer, D. M.; Shao, H. H. *J. Chem. Phys.* **1995**, *98*, 5809.
(20) Sumpter, B. G.; Noid, D. W.; Wunderlich, B. *J. Chem. Phys.* **1990**, *93*, 6875.
(21) Noid, D. W.; Sumpter, B. G.; Wunderlich, B. *Macromolecules* **1990**, *23*, 664.
(22) Liang, G. L.; Noid, D. W.; Sumpter, B. G.; Wunderlich, B. *J. Polym. Sci. Ploym. Phys. Ed.*, **1993**, *31*, 1909.
(23) Pennings, A. J.; Zwijnenburg, A. *J. Polym. Sci. Polym. Phys. Ed.*, **1979**, *17*, 1011.
(24) Snook, J.; Pennings, A. J. *Colloid Polym. Sci.* **1984**, *262*, 712.
(25) Lemstra, P. J.; van Aerle, N. A. J. M.; Bastiaansen, C. W. M. *Polym. J.* **1987**, *19*, 85.
(26) Kyotani, H.; Tanabe, Y. *Kobunshi Ronbunshu (Polym. Chem.)* **1989**, *46*, 51.
(27) van Aerle, N. A. J. M.; Lemstra, P. J.; Braam, A. W. M. *Polym. Commun.* **1989**, *30*, 7.
(28) Murthy, N. S.; Correale, S. T.; Kavesh, S. *Polym. Commun.* **1990**, *31*, 50.
(29) Smith, P.; Lemstra, P. J.; Pijpers, J. P. L.; Kiel, A. M. *Colloid Polym. Sci.* **1981**, *259*, 1070.
(30) Matsuo, M.; Inoue, K.; Abumiya, N. *Sen-i Gakkaishi* **1984**, *40*, T-275.
(31) Cho, Y., Kobayashi, M., Tadokoro, H. *Polym. Prepr. Jpn.* **1986**, *30*, 1842.

MA960333+